Journal of Alloys and Compounds 519 (2012) 77–81

Contents lists available at SciVerse ScienceDirect

Journal of Alloys and Compounds

journal homepage: www.elsevier.com/locate/jallcom

Interface strain coupling and its impact on the transport and magnetic properties of $LaMnO_3$ thin films grown on ferroelectrically active substrates

R.K. Zheng[a,b,*], Y. Wang[b], H.-U. Habermeier[c], H.L.W. Chan[b], X.M. Li[a], H.S. Luo[a]

[a] State Key Laboratory of High Performance Ceramics and Superfine Microstructure, Shanghai Institute of Ceramics, Chinese Academy of Sciences, Shanghai 200050, China
[b] Department of Applied Physics and Materials Research Center, The Hong Kong Polytechnic University, Hong Kong, China
[c] Max Planck Institute for Solid State Research, Heisenbergstrasse 1, D-70569 Stuttgart, Germany

ARTICLE INFO

Article history:
Received 24 September 2011
Received in revised form
11 December 2011
Accepted 12 December 2011
Available online 27 December 2011

Keywords:
Thin film
Electronic properties
Magnetoresistance
PMN-PT single crystal

ABSTRACT

Thin films of $LaMnO_3$ have been epitaxially grown on ⟨0 0 1⟩ oriented ferroelectric $0.67Pb(Mg_{1/3}Nb_{2/3})O_3$-$0.33PbTiO_3$ (PMN-PT) single-crystal substrates. The poling of the PMN-PT crystal causes a decrease in the resistance and an increase in the magnetization and magnetoresistance of the $LaMnO_3$ film. *In situ* X-ray diffraction measurements revealed that these changes arise from the poling-induced strain in the PMN-PT substrate, which reduces the in-plane tensile strain and the Jahn–Teller (JT) distortion of MnO_6 octahedra of the $LaMnO_3$ film. Moreover, it was found that the transport properties of $LaMnO_3$ films are much more sensitive to the poling-induced strain than that of $CaMnO_3$ films for which there is no JT distortion, implying that the electron–lattice coupling is one of the most important ingredients in understanding the strain effect in $LaMnO_3$ films.

1. Introduction

The discovery of colossal magnetoresistance phenomenon [1,2] has rekindled the interest in perovskite manganites of general formula $La_{1-x}A_xMnO_3$ (A = Ca, Sr, Ba). The $LaMnO_3$ is the end member of this class of materials and shows large cooperative Jahn–Teller (JT) distortion of MnO_6 octahedra, $d_{3x^2-r^2}/d_{3y^2-r^2}$ orbital ordering, and A-type antiferromagnetic spin ordering [3]. A number of theoretical and experimental studies have shown that the JT distortion, orbital ordering, structural, transport, and magnetic properties of $LaMnO_{3+\delta}$ are particularly sensitive to oxygen nonstoichiometry δ [4–10]. Any slight oxygen overdoping (e.g., $\delta = 0.01$) would cause a portion of Mn^{3+} ions to be oxidized to Mn^{4+} ions, causing dramatic changes in the JT distortion, structural, transport, and magnetic properties [7–10]. Although we have studied the effects of the substrate-induced strain on the electrical and magnetic properties of oxygen overdoped $LaMnO_{3+\delta}$ ($\delta \sim 0.09$) films [6] whose electrical transport properties are quite similar to that of hole doped $La_{1-x}Ca_xMnO_3$ ($0.15 \leq x \leq 0.2$) compounds, the intrinsic effects of substrate-induced strain on the $LaMnO_{3+\delta}$ ($\delta \geq 0$) film are still not well understood. Since the $LaMnO_3$ is the parent compound of doped perovskite manganites, a detailed study of the effects of substrate-induced strain on the electrical transport and magnetic properties of oxygen stoichiometry $LaMnO_3$ films, whose electrical transport properties are very different from those of oxygen overdoped $LaMnO_{3+\delta}$ ($\delta \sim 0.09$) films [6], is highly desired in order to obtain a more comprehensive understanding of the essential physics of perovskite manganites.

A number of experimental work have demonstrated that the strain state, electrical, and magnetic properties of perovskite manganite thin films can be reversibly and dynamically modulated via the ferroelectric poling effect or the converse piezoelectric effect of ferroelectric $(1-x)Pb(Mg_{1/3}Nb_{2/3})O_3$-$xPbTiO_3$ single crystals [11–15]. In this work, we epitaxially grown oxygen almost stoichiometry $LaMnO_3$ films on ferroelectric $0.67Pb(Mg_{1/3}Nb_{2/3})O_3$-$0.33PbTiO_3$ (PMN-PT) single-crystal substrates and studied the impact of the substrate-induced strain on the electrical and magnetic properties of the $LaMnO_3$ film by *in situ* modifying the strain state of the $LaMnO_3$ film, so that the effects of oxygen nonstoichiometry on the properties of the $LaMnO_3$ film could be kept constant. Due to the epitaxial nature of the interface, the poling-induced strain was effectively transferred to the $LaMnO_3$ film, causing significant changes in the JT distortion, resistance, magnetization, and magnetoresistance (MR). An analysis of the overall experimental results shows that the electronic phase separation and the coupling of electrons to JT distortion of MnO_6 octahedra are crucial to understand the strain-property coupling effects in manganite films.

* Corresponding author at: State Key Laboratory of High Performance Ceramics and Superfine Microstructure, Shanghai Institute of Ceramics, Chinese Academy of Sciences, Shanghai 200050, China. Tel.: +86 21 52411205; fax: +86 21 52413122.
E-mail address: zrk@ustc.edu (R.K. Zheng).

0925-8388/$ – see front matter © 2011 Elsevier B.V. All rights reserved.
doi:10.1016/j.jallcom.2011.12.099

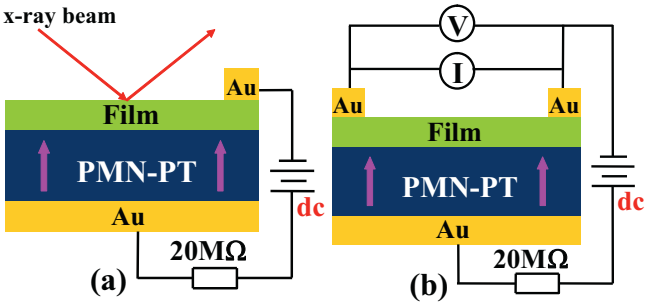

Fig. 1. Schematic diagrams of the film/PMN-PT structure and the configuration for *in situ* measurements of the strain (a) and the resistance (b). The arrow in the PMN-PT represents the poling direction.

2. Experimental details

High quality PMN-PT single crystals were grown from melt by a modified Bridgman technique [16]. $LaMnO_3$ and $CaMnO_3$ films were deposited on polished PMN-PT single-crystal substrates by pulsed laser deposition using a 248 nm KrF excimer laser with a repetition rate of 4 Hz. Both the $LaMnO_3$ and $CaMnO_3$ films were deposited at 700 °C with the oxygen pressure fixed at 200 mTorr. After deposition, these films were *in situ* cooled to room temperature. $CaMnO_3$ films were further postannealed in air at 700 °C for 30 min using a rapid thermal processor furnace to reduce oxygen deficiencies. No further postannealing was made for $LaMnO_3$ films in order to avoid oxygen overdoping.

X-ray diffraction (XRD) patterns of the $LaMnO_3$ and $CaMnO_3$ films were recorded using a four-circle Bruker D8 Discover X-ray diffractometer equipped with a four-bounce Ge(2 2 0) monochromator. Fig. 1(a) shows a schematic diagram for *in situ* measurements of the poling-induced strain in the $LaMnO_3$ and $CaMnO_3$ films using XRD. Electric potentials were applied to the PMN-PT substrate through the bottom gold electrode and the top $LaMnO_3$ (or $CaMnO_3$) film during XRD θ–2θ scans.

Fig. 1(b) shows the resistance measurement circuit for the $LaMnO_3$/PMN-PT and $CaMnO_3$/PMN-PT structures. A Physical Property Measurement System (PPMS 9T, Quantum Design) was employed to measure the resistance of the $LaMnO_3$ film between the two top-top gold electrodes with magnetic fields up to $H = 9$ T applied parallel to the film plane. The magnetic properties of the $LaMnO_3$ film were recorded using a superconducting quantum interference device (SQUID-VSM 7T, Quantum Design) magnetometer with a magnetic field of $H = 500$ Oe applied parallel to the film plane.

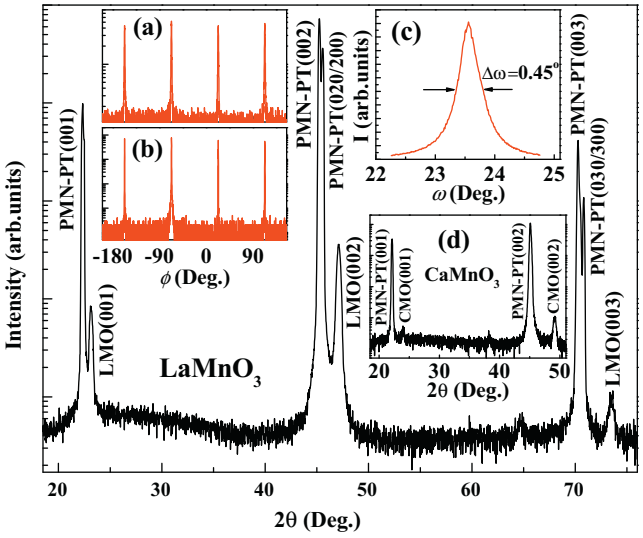

Fig. 2. XRD pattern of the $LaMnO_3$/PMN-PT structure. The insets (a) and (b) show the XRD phi scans of the $LaMnO_3$(1 0 1) and PMN-PT(1 0 1) planes, respectively. The inset (c) shows the XRD rocking curve taken around the $LaMnO_3$(0 0 2) reflection. The inset (d) shows the XRD pattern of the $CaMnO_3$/PMN-PT structure. Note that the LMO and CMO represent the $LaMnO_3$ film and the $CaMnO_3$ film, respectively.

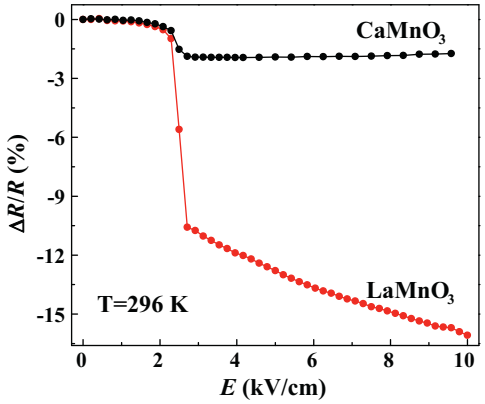

Fig. 3. Electric-field-induced relative changes in the resistance of the $LaMnO_3$ and $CaMnO_3$ films at 296 K as a function of the electric field (E) applied to the PMN-PT substrate.

3. Results and discussion

Fig. 2 shows the XRD θ–2θ scan of the $LaMnO_3$/PMN-PT structure. One can see that (0 0 l) (l = 1, 2, 3) and (0 l 0)/(l 0 0) (l = 2, 3) diffraction peaks from the PMN-PT substrate appear, indicating that the ferroelectric domains in the PMN-PT substrate are mainly *c*-axis preferentially oriented while some of domains are *a*- or *b*-axis oriented. Moreover (0 0 l) (l = 1, 2, 3) diffraction peaks from the $LaMnO_3$ film can also be observed, implying that the $LaMnO_3$ film is *c*-axis preferentially oriented. No diffraction peaks were detected that would be indicative of secondary phases. We have performed XRD phi scans of the $LaMnO_3$(1 0 1) and PMN-PT(1 0 1) planes and observed sharp fourfold symmetrical diffraction peaks originating from the $LaMnO_3$ film and the PMN-PT substrate [the inset (a) and (b) of Fig. 2], respectively, indicating that the $LaMnO_3$ film has been epitaxially grown on the PMN-PT substrate. XRD rocking curve taken around the $LaMnO_3$(0 0 2) diffraction peak has a full width at half maximum of ~0.45° [the inset (c) of Fig. 2], implying good crystalline quality of the $LaMnO_3$ film. The XRD θ–2θ scan performed on the $CaMnO_3$/PMN-PT structure shows that the $CaMnO_3$ film is highly *c*-axis preferentially oriented and has no secondary phases [the inset (d) of Fig. 2]. The out-of-plane lattice constants c of the $LaMnO_3$ and $CaMnO_3$ films, calculated from the out-of-plane θ–2θ scan data, are 3.8545 Å and 3.705 Å, respectively. These values are smaller than those of the corresponding bulk materials [17,18], implying that both the $LaMnO_3$ film and the $CaMnO_3$ film are subjected to biaxial in-plane tensile strain. The strain states of these films are consistent with the fact the lattice constants of both the $LaMnO_3$ and the $CaMnO_3$ bulk materials are much smaller than those ($a \sim b \sim c \sim 4.02$ Å [19]) of the PMN-PT crystal.

Fig. 3 shows the electric-field-induced relative change in the resistance, $\Delta R/R$ $\left[\Delta R/R = [R(E) - R(0)]/R(0)\right]$, for the $LaMnO_3$ and $CaMnO_3$ films as a function of the electric field E applied to the PMN-PT substrate. It should be pointed out that, initially, the PMN-PT substrate was in the unpoled state (denoted by P_r^0). The resistance for both the $LaMnO_3$ film and the $CaMnO_3$ film are almost field-independent for $E \leq 2$ kV/cm but decreases remarkably in the field region of 2.3 kV/cm < E < 2.7 kV/cm, where the poling of the PMN-PT substrate occurs as estimated from the polarization-electric field loop of the PMN-PT substrate [20]. Such a field-induced decrease in the resistance is similar to that observed in the oxygen overdoped $LaMnO_{3+\delta}$/PMN-PT [6] and $La_{0.7}Ca_{0.15}Sr_{0.15}MnO_3$/PMN-PT [21] structures and could be ascribed to the change in the strain state of the films induced by the poling-induced strain in the PMN-PT substrate. To clarify this point, we performed a series of *in situ* XRD θ–2θ scans by applying electric fields to the PMN-PT substrate. Selected XRD patterns in the vicinity of the (0 0 2) diffraction peaks

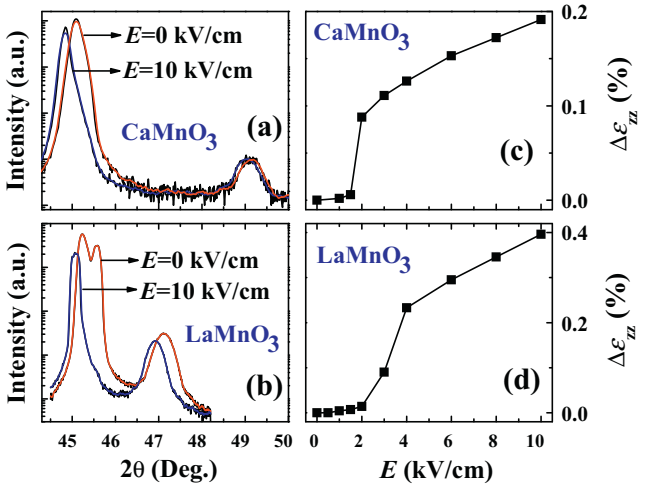

Fig. 4. XRD patterns in the vicinity of (0 0 2) diffraction peaks under $E = 0$ and 10 kV/cm for the $CaMnO_3$ film (a) and the $LaMnO_3$ film (b). (c) and (d) show the electric-field-induced strain $\Delta\varepsilon_{zz}$ as a function of E for the $CaMnO_3$ film and the $LaMnO_3$ film, respectively.

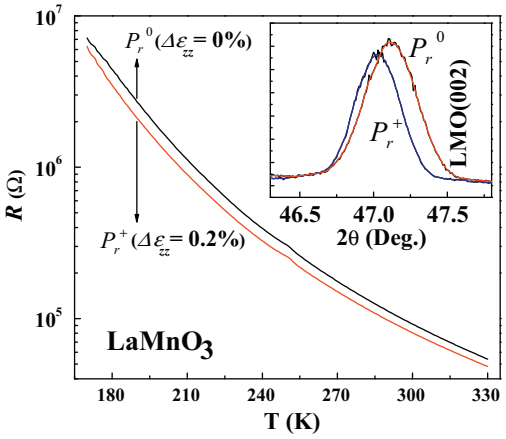

Fig. 5. Temperature dependence of the resistance for the $LaMnO_3$ film when the PMN-PT substrate was in the P_r^0 state and the P_r^+ state, respectively. The inset shows the XRD patterns in the vicinity of $LaMnO_3$(0 0 2) diffraction peak when the PMN-PT substrate was in the P_r^0 state and the P_r^+ state, respectively.

under $E = 0$ and 10 kV/cm are shown in Fig. 4(a) and (b), respectively. It can be seen that the (0 0 2) diffraction peaks of the PMN-PT substrate and the $CaMnO_3$ (or $LaMnO_3$) film shift toward lower 2θ angle under $E = 10$ kV/cm, implying that the lattice constants c of both the substrate and the film are larger than those under $E = 0$ kV/cm. For $LaMnO_3$/PMN-PT structure, the (0 2 0)/(2 0 0) diffraction peak near $2\theta = 45.58^\circ$ disappears under $E = 10$ kV/cm, indicating that the electric field induces a- and (or) b-axis oriented ferroelectric domains rotate toward c-axis. The induced out-of-plane strain $\Delta\varepsilon_{zz}$ [$\Delta\varepsilon_{zz} = [c(E) - c(0)]/c(0)$] for the $CaMnO_3$ film and the $LaMnO_3$ film are shown in Fig. 4(c) and (d), respectively. $\Delta\varepsilon_{zz}$ increases significantly near the coercive field of the PMN-PT substrate. It is known that the application of electric fields to an unpoled ferroelectric single crystal would induce a nonlinear change in the strain along the field direction near the coercive field of the crystal due to the rotation of polarization direction of ferroelectric domains toward the field direction [22]. The nonlinear increase in $\Delta\varepsilon_{zz}$ gives strong evidence that the poling-induced strain has been effectively transferred to the $CaMnO_3$ and $LaMnO_3$ films.

We note that the $\Delta R/R$ of the $CaMnO_3$ film is much smaller than that of the $LaMnO_3$ film. For example, the $\Delta R/R$ and the $\Delta\varepsilon_{zz}$ under $E = 4$ kV/cm for the $LaMnO_3$ film are ~11.9% and ~0.233%, respectively. The sensitivity of the relative change in the resistance to the induced out-of-plane strain, characterized by $(\Delta R/R)/(\Delta\varepsilon_{zz})$, is calculated to be ~51.1. This value is close to that (~43.5) for the $La_{0.7}Ca_{0.15}Sr_{0.15}MnO_3$ thin film near the insulator-to-metal transition temperature (T_P) where a strong coupling of electrons to the JT distortion of MnO_6 octahedra was observed [21,23]. However, for the $CaMnO_3$ film, the $(\Delta R/R)/(\Delta\varepsilon_{zz})$ under $E = 4$ kV/cm is only ~15.2. This value is much smaller than that of the $LaMnO_3$ film, showing that the transport properties of the $LaMnO_3$ film are much more sensitive to the lattice strain than that of the $CaMnO_3$ film. As is known, the $CaMnO_3$ film does not show JT distortion since all manganese ions are Mn^{4+} so the effects of the electron–lattice coupling stemming from the JT distortion on the transport properties can be discarded. Therefore, it is believed that the decrease in the resistance of the $CaMnO_3$ film near the coercive of the PMN-PT substrate is probably caused by the increase in the electronic bandwidth due to the reduction in the in-plane tensile strain, which could lead to changes in the Mn—O bond length [24]. In contrast, the $LaMnO_3$ film shows a large JT distortion of MnO_6 octahedra [2] which are known to highly influence the transport and magnetic properties. Using X-ray absorption near edge structure, Souza-Neto et al. [24] found that the substrate-induced in-plane tensile strain causes the MnO_6 octahedra to be compressed in the direction perpendicular to the film plane and elongated in the direction parallel to the film plane. It is, thus, expected that the poling-induced decrease in the in-plane tensile strain would reduce the JT distortion of MnO_6 octahedra of the $LaMnO_3$ film and thus favors the active hopping of electrons. According to Millis et al. [25], the JT strain (ε_{JT}) for manganite films could be expressed as [$\varepsilon_{JT} = 1/2(\varepsilon_{zz} - \varepsilon_{xx})$] where ε_{zz} and ε_{xx} are the out-of-plane strain and in-plane strain, respectively. Assuming approximately volume preservation distortion, the relationship between the change in the JT distortion $\Delta\varepsilon_{JT}$ and $\Delta\varepsilon_{zz}$ can be written as $\Delta\varepsilon_{JT} = -0.75\Delta\varepsilon_{zz}$. Using the measured $\Delta\varepsilon_{zz}$ for the $LaMnO_3$ film, it is roughly estimated that the JT distortion of the $LaMnO_3$ film decreases by ~0.3% when $E = 10$ kV/cm is applied to the PMN-PT substrate.

Fig. 5 shows the temperature dependence of the resistance for the $LaMnO_3$ film when the PMN-PT substrate was in the P_r^0 state and the poled state (denoted by P_r^+), respectively. For the P_r^0 state, the resistance of the $LaMnO_3$ film increases with decreasing temperature from 330 K to 170 K. For $T < 170$ K, the film is highly insulating. After measuring the resistance as a function of temperature for the P_r^0 state, we *in situ* poled the PMN-PT substrate by applying an electric filed of $E = 10$ kV/cm to the PMN-PT substrate at room temperature. After the PMN-PT substrate had been poled to the P_r^+ state, we turned off the poling field. Since the ferroelectric Curie temperature ($T_C \sim 430$ K) of the PMN-PT substrate is much higher than room temperature, the polarization direction of ferroelectric domains would remain toward the field direction (i.e. along the ⟨0 0 1⟩ direction) after turning off the poling field. A remnant in-plane compressive strain is, thus, induced in the PMN-PT substrate, which is subsequently transferred to the epitaxial $LaMnO_3$ film, thereby causing a reduction in the in-plane tensile strain of the $LaMnO_3$ film. This is reflected by the shift of the $LaMnO_3$(0 0 2) diffraction peak to lower 2θ angle, as shown in the inset of Fig. 5. The 2θ angle shifts from 47.12° to 47.02°, corresponding to an increase in the lattice constant c from 3.854 to 3.862 Å. The out-of-plane strain ε_{zz} [$\varepsilon_{zz} = (c_{film} - c_{bulk})/c_{bulk}$] of the $LaMnO_3$ film is calculated to be reduced from −1.33% to −1.13% (i.e., $\Delta\varepsilon_{zz} = 0.2\%$). Assuming approximate volume preserving distortion of the film, an increase in $\Delta\varepsilon_{zz}$ by 0.2% would lead to a decrease in ε_{xx} by 0.1% (i.e., $\Delta\varepsilon_{xx} = -0.1\%$). Such a decrease in the in-plane tensile strain significantly affects the transport properties of the $LaMnO_3$ film. It can be seen that, associated with the switching of the poling state from P_r^0 to P_r^+, the resistance decreases in the whole

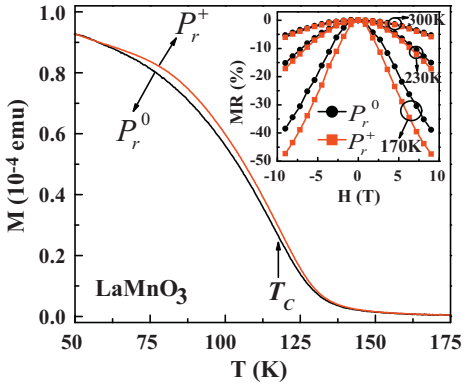

Fig. 6. Temperature dependence of the magnetization for the $LaMnO_3$ film when the PMN-PT substrate was in the P_r^0 state and the P_r^+ state, respectively. The inset shows the MR versus H curves at several fixed temperatures.

temperature range between 170 K and 330 K. The relative change in the resistance $\Delta R/R$, defined as $\Delta R/R = [R(P_r^0) - R(P_r^+)]/R(P_r^0)$, is ~12.5% at 296 K and increases to ~22.5% at 185 K. Similar to the mechanism accountable for the electric-field-induced decrease in the resistance near the coercive field of the PMN-PT discussed above, the decrease in the resistance in the temperature range between 170 K and 330 K is clearly due to the poling-induced strain which increases the electronic bandwidth and weakens the electron–lattice coupling strength as a result of suppressed JT distortion.

We found that the poling-induced strain has a considerable impact on the MR [MR = $[R(H) - R(0)]/R(0)$] of the $LaMnO_3$ film. The inset of Fig. 6 shows the MR versus H curves at T = 170, 230, and 300 K when the PMN-PT substrate was in the P_r^0 and P_r^+ state, respectively. The results clearly show that in comparison with the MR when the PMN-PT substrate was in the P_r^0 state, the MR value at any fixed temperature when the PMN-PT substrate was in the P_r^+ state is enhanced for any fixed H value. For example, at H = 9 T associated with the poling of the substrate, the MR at T = 170, 230, and 300 K was enhanced by ~22.2%, 13.7%, and 11%, respectively, indicating that the lower the temperature, the larger the effects of the induced strain on the MR. This strain-induced enhancement of MR is similar to that observed in the $La_{7/8}Ba_{1/8}MnO_3$ films grown on PMN-PT substrates [26], implying that the underlying mechanism responsible for the enhancement of MR is probably the same as that in the $La_{7/8}Ba_{1/8}MnO_3$/PMN-PT structure. Namely, the effects of the induced strain on MR are closely related to the strain-induced change in the volume fraction of coexisting paramagnetic and ferromagnetic phases. Fig. 6 shows the normalized zero-field-cooled magnetization as a function of temperature for the $LaMnO_3$ film when the PMN-PT substrate was in the P_r^0 and P_r^+ state, respectively. Associated with the poling of the PMN-PT substrate, the magnetization (M) was enhanced considerably. At $T_c \sim 118$ K, the poling-induced relative change in the magnetization, $\Delta M/M$, is ~12.2%. Although the magnetic ground state is ferromagnetic (FM), the $LaMnO_3$ film is highly insulating at low temperatures. It is, possible that a very small portion of Mn^{3+} ions could have been oxidized to Mn^{4+} ions, resulting in local Mn^{3+}–O–Mn^{4+} double-exchange (DE) interaction. Due to the DE interaction, a very small fraction of FM clusters may form at low temperature and are embedded in the Mn^{3+}–O–Mn^{3+} antiferromagnetically coupled insulating matrix, giving rise to the FM insulating behavior of the resistance at low temperatures (T < 118 K). At high temperatures (T > 118 K), although short range FM ordering within FM clusters is not established, a small fraction of FM clusters may still exist because of local Mn^{3+}–O–Mn^{4+} DE interaction. Associated with the increase in the electronic bandwidth and the suppression of the JT distortion induced by the poling of the PMN-PT substrate, the volume fraction of the FM clusters would increase while that of the PM insulating matrix would decrease [26]. As a result, the MR for the P_r^+ state is larger than that for the P_r^0 state due to enhanced volume fraction of FM clusters.

4. Summary

We have studied the intrinsic effects of the ferroelectric poling-induced strain on the strain state, JT distortion, electrical resistance, magnetoresistance, and magnetic properties of $LaMnO_3$ films grown on PMN-PT substrates. The poling of the PMN-PT substrate reduces the in-plane tensile strain and hence the JT distortion ($\Delta\varepsilon_{JT}$) of the $LaMnO_3$ film, giving rise to a decrease in the resistance and an increase in the magnetization and magnetoresistance. These effects were qualitatively explained within the framework of strain-induced decrease in the JT electron–lattice coupling and increase in the electron bandwidth. Moreover, we found that the transport properties of $LaMnO_3$ films are much more sensitive to the induced lattice strain than that of $CaMnO_3$ films, implying that the JT electron–lattice coupling are crucial to understand the strain effect in $LaMnO_3$ films.

Acknowledgments

This work was supported by NSFC/RGC (Grant No. N_PolyU501/08), PolyU internal grant G-U846 and the Center for Smart Materials of the Hong Kong Polytechnic University, the Max Planck Institute for Solid State Research, the National Basic Research Program of China (973 Program, Grant No. 2009CB623304), and the National Science Foundation of China (Grant No. 90922026, 11090332).

References

[1] S. Majumdar, H. Huhtinen, H.S. Majumdar, P. Paturi, J. Alloys Compd. 512 (2012) 332.
[2] J.C. Debnath, R. Zeng, J.H. Kim, P. Shamba, D.P. Chen, S.X. Dou, J. Alloys Compd. 510 (2012) 125.
[3] J. Rodríguez-Carvajal, M. Hennion, F. Moussa, A.H. Moudden, L. Pinsard, A. Revcolevschi, Phys. Rev. B 57 (1998) R3189.
[4] L. Morales, J. Rodríguez-Carvajal, A. Caneiro, J. Alloys Compd. 369 (2004) 97.
[5] P. Orgiani, C. Aruta, R. Ciancio, A. Galdi, L. Maritato, Appl. Phys. Lett. 95 (2009) 013510.
[6] R.K. Zheng, H.-U. Habermeier, H.L.W. Chan, C.L. Choy, H.S. Luo, Phys. Rev. B 81 (2010) 104427.
[7] K.-Y. Choi, Y.G. Pashkevich, V.P. Gnezdilov, G. Güntherodt, A.V. Yeremenko, D.A. Nabok, V.I. Kamenev, S.N. Barilo, S.V. Shiryaev, A.G. Soldatov, P. Lemmens, Phys. Rev. B 74 (2007) 064406.
[8] R. Horyn, A.J. Zaleski, E. Bukowska, A. Sikora, J. Alloys Compd. 383 (2004) 80.
[9] A. Dubey, V.G. Sathe, R. Rawat, J. Appl. Phys. 104 (2008) 113530.
[10] S.N. Barilo, V.I. Gatal'skaya, S.V. Shiryaev, G.L. Bychkov, L.A. Kurochkin, S.N. Ustinovich, R. Szymczak, M. Baran, B. Krzymánska, Phys. Solid State 45 (2003) 146.
[11] C. Thiele, K. Dörr, O. Bilani, J. Rödel, L. Schultz, Phys. Rev. B 74 (2007) 054408.
[12] C. Thiele, K. Dörr, S. Fähler, L. Schultz, D.C. Meyer, A.A. Levin, P. Paufler, Appl. Phys. Lett. 87 (2005) 262502.
[13] M.C. Dekker, A. Herklotz, L. Schultz, M. Reibold, K. Vogel, M.D. Biegalski, H.M. Christen, K. Dörr, Phys. Rev. B 84 (2011) 054463.
[14] E.J. Guo, J. Gao, H.B. Lu, EPL 95 (2011) 47006.
[15] Q.P. Chen, J.J. Yang, Y.G. Zhao, S. Zhang, J.W. Wang, M.H. Zhu, Y. Yu, X.Z. Zhang, Z. Wang, B. Yang, D. Xie, T.L. Ren, Appl. Phys. Lett. 98 (2011) 172507.
[16] R.K. Zheng, S.H. Choy, Y. Wang, H.L.W. Chan, C.L. Choy, H.S. Luo, J. Alloys Compd. 509 (2011) 4878.
[17] M. Tovar, G. Alejandro, A. Butera, A. Caneiro, M.T. Causa, F. Prado, R.D. Sánchez, Phys. Rev. B 60 (1999) 10199.
[18] Z. Zeng, M. Greenblatt, M. Croft, Phys. Rev. B 59 (1999) 8784.
[19] B. Noheda, D.E. Cox, G. Shirane, J. Gao, Z.-G. Ye, Phys. Rev. B 66 (2002) 054104.
[20] R.K. Zheng, Y. Jiang, Y. Wang, H.L.W. Chan, C.L. Choy, H.S. Luo, Phys. Rev. B 79 (2009) 174420.

[21] R.K. Zheng, H.-U. Habermeier, H.L.W. Chan, C.L. Choy, H.S. Luo, Phys. Rev. B 80 (2009) 104433.
[22] B. Jaffe, W.R. Cook Jr., H. Jaffe, Piezoelectric Ceramics, Academic Press, New York, 1971.
[23] Y. Moritomo, A.A. Asamitsu, Y. Tokura, Phys. Rev. B 56 (1997) 12190.
[24] N.M. Souza-Neto, A.Y. Ramos, H.C.N. Tolentino, E. Favre-Nicolin, L. Ranno, Phys. Rev. B 70 (2004) 174451.
[25] A.J. Millis, T. Darling, A. Migliori, J. Appl. Phys. 83 (1998) 1588.
[26] R.K. Zheng, Y. Wang, H.L.W. Chan, C.L. Choy, H.-U. Habermeier, H.S. Luo, J. Appl. Phys. 108 (2010) 033912.